www.czasopisma.pan.pl PAN POLSKA AKADEMIA NAUK www.journals.pan.pl

A R C H I V E S O F M E T A L L U R G Y A N D M A T E R I A L S

Volume 60 2015 Issue 4

DOI: 10.1515/amm-2015-0453

D. WOŹNIAK*,#, M. HOJNY*, T. GĄDEK**, M. GŁOWACKI*,***

NUMERICAL AND EXPERIMENTAL FORMING OF AXISYMMETRIC PRODUCTS USING METHODS OF DEEP DRAWING AND FLOW FORMING

NUMERYCZNE I EKSPERYMENTALNE KSZTAŁTOWANIE WYROBÓW OSIOWOSYMETRYCZNYCH METODĄ TŁOCZENIA ORAZ KSZTAŁTOWANIA OBROTOWEGO

The paper deals with the problem of forming of axisymmetric element. Two-stages process was taken into consideration: deep drawing of metal blank using hydraulic press and the method of elongating flow forming. The contribution presents results of numerical and experimental analyzes. Numerical simulations of both the processes were realized in Kraków at AGH University. Numerical verification of both processes was carried out using finite element models implemented with the help of commercial analysis system on basis of conducted in Poznań experimental shaping tests of Hastelloy C-276 alloy. The tests were aimed to find opportunities and conditions of plastic deformation of the material. This article summarizes example results of both numerical and experimental forming of products made of hard-to-deform material..

Keywords: deep drawing, flow forming, FEM modeling, hard-to-deform material

W artykule przedstawiono zagadnienie dotyczące formowania produktów osiowosymetrycznych. Proces został podzielony na dwa etapy: głębokie tłoczenie z wykorzystaniem prasy hydraulicznej oraz kształtowania obrotowego wydłużającego. Przedstawione zostały zarówno wyniki analiz numerycznych jak i badań eksperymentalnych. Analizy numeryczne wykonane zostały w AGH, natomiast badania eksperymentalne w Instytucie Obróbki Plastycznej w Poznaniu. Materiałem wejściowym do badań był Hastelloy C-276. Przeprowadzone badania ukierunkowane były na określeniu możliwości kształtowania wyrobów osiowosymetrycznych z materiałów trudno odkształcalnych.

1. Introduction

The growing demand for products with higher durability and quality of performance affects the need for new technologies and for new methods of analysis of the correctness of their performance at the design stage [1-3]. Continuous progress in the field of rotary plastic forming methods affects, inter alia, the classification of technological processes. More and more often used technique of forming of axisymmetric products is rotary forming which includes metal spinning, flow forming and hybrid forming. The rotary forming processes is classified among stamping, however, the forces encountered during spinning and flow forming are much smaller due to the local contact of tools with shaped material [4,5]. The most important difference between the metal spinning and the flow forming concerns the product wall thickness. In spinning process, the thickness remains the same, while in the flow forming it is intentionally reduced. Rotary forming can be performed in the cold and hot state. Material deformation in the process of metal spinning is influenced by many factors [6-8]. The most important are:

- rotational speed of the mandrel
- working roller travel
- working radius of the roller
- diameter of the metal spinning roller
- sheet disk thickness
- the disk diameter

The use of modern computer technology has become an integral part of the development of innovative stamping, spinning and flow forming technologies. The application of numerical analysis systems based on the finite element method speeds up the design and optimization of forming processes. However, the use of computer simulation systems with GUI for analysis of rotary forming is complicated, mainly due to the lack of a commercial software dedicated to such processes and equipped with system of process automation. An increasing number of manually operated numerical analyzes of the rotary forming process shows how important is that method of metal forming [9,10] in the context of industrial processes.

The basis of the analysis were tests carried out in Metal Forming Institute in Poznan. The test material, a Hastelloy C-276 (UNS N10276) alloy, was subjected to stamping and subsequent

* AGH UNIVERSITY OF SCIENCE AND TECHNOLOGY, FACULTY OF METALS ENGINEERING AND INDUSTRIAL COMPUTER SCIENCE, AL. A. MICKIEWICZA 30, 30-059 KRAKÓW, POLAND

** METAL FORMING INSTITUTE, JANA PAWŁA II 14, 61-139 POZNAN, POLAND

*** THE JAN KOCHANOWSKI UNIVERSITY (JKU), KIELCE

Correesponding author: dwozniak@agh.edu.pl

flow forming. Hastelloy C-276 is an alloy of nickel, chrome, and molybdenum, with an average nickel content of about 57%. It exhibits a significant resistance to corrosion in various chemical environments, including the presence of strong oxidizers like copper and iron chlorides, formic acid and seawater. Furthermore, it is characterized by great resistance to pitting and stress corrosion. Alloys with a nickel matrix are frequently used, among other , in the oil and natural gas extraction industry for parts of devices which are used for deep drilling and as a consequence are often exposed to corrosion [11].

In order to increase durability, nickel alloys are usually hardened through cold plastic deformation at temperatures which exclude recrystallization. The grains in a work-hardened metal are deformed, and the density of the dislocations is greater than in a annealed material. With the increase in cold plastic deformation, the material's hardness and durability increase, while its extension undergoes decrease [12].

The course of the flow forming process was designed on the basis of parameters published in the literature [13-16].

2. Numerical Modeling

2.1. Numerical model for deep drawing process

The geometrical modeling of the set of tools taking part in the FEM simulation has been developed with the use of CAD software. Main parts of the tool set, i.e.: punch, binder and die are presented in Fig. 1. Figure 2 shows a FEM-mesh model of the tools together with a blank. The blank was discretized using 64 nodal solid elements, which allow a very good accuracy of the calculations. The initial blank thickness was 2.0 mm. Three elements were applied along the material thickness.

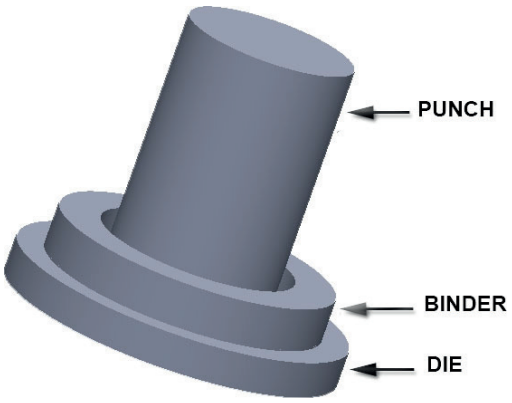

Fig. 1. CAD model of tools for deep drawing process

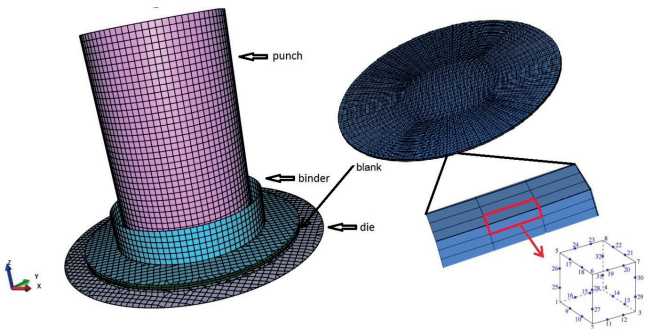

Fig. 2. FEM model of tools for deep drawing process

2.2. Numerical model of flow forming process

Fig. 3b shows finite elements discretization, as well as the positioning of the working tools and their resulting relation. Fig. 3a shows CAD model of tools before simplification of their geometry. The drawpiece has variable thickness and its side wall has variable shape. This results from the stamping operation performed prior to the flow forming process. The history of the material deformation comprises the history of deep drawing process, which was the first stage of the procedure. The mandrel rotates around its axis and, at the same time, it is a drive of cylindrical drawpiece giving it a rotational speed of 500 rpm. The forming rolls also rotate around their axes and additionally move along them. The movement speed of the rolls is equal to 5 mm/s.

Properties of the blank material adopted from the available literature and solver database are as follows:

- Young's modulus: 2.02 x 10^5 MPa,
- Poisson ratio:0.31,
- density: 8.22 x 10^3 kg/m^3.

The yield stress curve has been calculated on the basis of data included in solver database, as well. After the tool set was prepared the FEM-mesh model of flow forming simulation was ready to simplification. Surfaces, which didn't take part in the process were removed from the model. These areas have undefined contact with the material. Such operation allows reduction of the simulation time without influence on very good calculation accuracy in case of deep drawing.

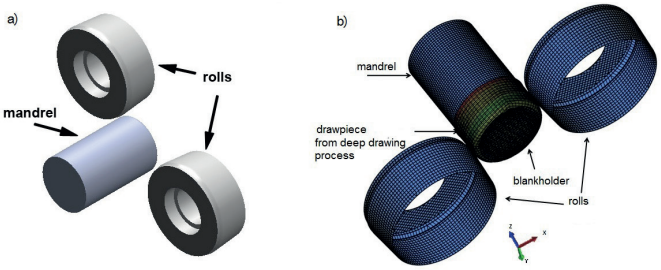

Fig. 3. Model of tools for flow forming process a) CAD model, b) FEM mesh

The compressibility of the material was modelled with the use of penalty for deflection from stiffness. The adopted value of penalty coefficient responsible for the stiffness had value of 10^4. It means that we allow for small penetrations between the surfaces being in contact. A contact pressure, proportional to the penetration distance, was applied to keep the bodies separated. This assumption results in release of contact at the interface between the material and tools (Fig 4). At the same time the accuracy of the calculation is maintained and the computation time is reduced.

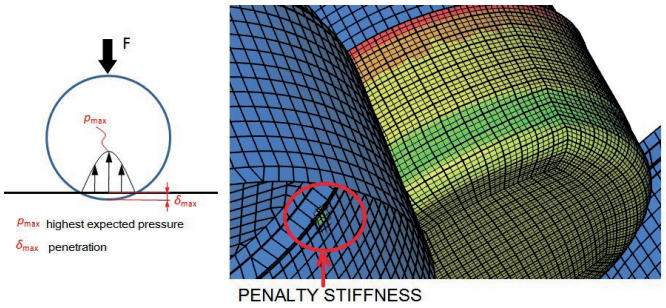

Fig. 4. Penetration area at the interface between the tools and material

3. Experimental tests

3.1. Tested material

The samples for testing have shape of disks made of Hastelloy C-276 sheet metal, cut with a water jet. The diameter of each disk was 200 mm and its thickness 2 mm. The hardness of disks in their initial state was 53 HRA on average. The chemical composition of Hastelloy C-276 alloy is presented in Table 1.

TABLE 1

Chemical composition of the Hastelloy C-276 alloy

Ni	Mo	Cr	Fe	W	Mn	Co	C	S
57.1	16.2	16,1	6.05	3.40	0.5	0.5	0.003	0.002

This alloy is characterized by a strong tendency towards strengthening during plastic deformation. Its yield strength $R_{0,2}$ was equal to 405 MPa, tensile strength R_m equal to 765 MPa, and a minimum elongation to rupture A5 equal to 62% [11].

The tests were conducted at testing stations which included a PYE-250 hydraulic press with 2500 kN of compression force and an MZH-400 flow forming machine. A die appropriate for cylindrical stamping was used for tests on the PYE-250 press, while a cylindrical mandrel and a set of forming rollers with a 30° angle of attack were used for elongative flow-forming tests.

3.2. Methodology of studies

The tests were conducted in order to verify the possibility of plastic deformation of Hastelloy C-276 alloy during stamping process followed by elongation in flow forming process. The tests were conducted in the Metal Forming Institute in Poznan. The flow forming machine was numerically controlled and equipped with a cylindrical mandrel and two rollers.

The shapes and dimensions of the working parts of the die and stamp were adopted based on literature data [7-8]. A double press was used during tests of Hastelloy C-276 stamping. During the process of stamping, products with required shape were obtained, and subsequently transferred to flow-forming machine for elongation tests..

The elongation on flow-forming machine were conducted on 2 mm thick products of stamping process. The products obtained during stamping were not subjected to heat treatment before the flow-forming.

The flow-forming process was conducted with a tool traverse rate of 0.6 mm/rot and a 30% reduction in wall thickness.

The deformation in the direction of the wall's thickness was specified by formula (1):

$$\varepsilon = \frac{g_0 - g_1}{g_0} \cdot 100\% \tag{16}$$

where:
g_0 – thickness of the side wall before flow forming [mm]
g_1 – thickness of the side wall after flow forming [mm]

4. Example results from numerical analysis and experimental work

4.1. Stage 1 – deep drawing

During the stamping tests, the maximal force needed for stamping of a shaped product from 2 mm thick discs was found to be 598.2 kN for the maximal pressure binder force of 119.3 kN. The results of tests are presented in table 2. The wall thickness of the obtained product was measured and compared with results of numerical analysis. A significant increase in wall thickness was observed in the upper part of the product. Results of both numerical analysis and measurement are presented in Figures 5 and 6, respectively.

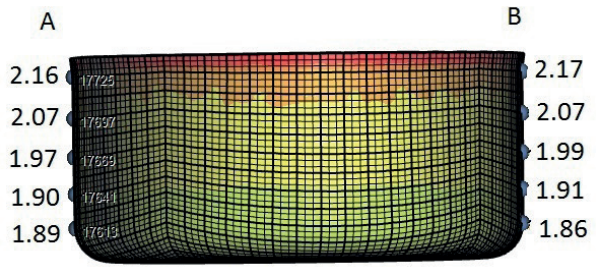

Fig. 5. Thickness distribution for final product after stamping process – numerical analysis. A, B – opposite sides of the product

TABLE 2

Dimensions of stamped products after the process of shaping (experimental and numerical results)

Stamped product dimensions							
Numerical analysis				Experimental work			
Outside diameter [mm]	Inside diameter [mm]	Average wall thickness [mm]	Height [mm]	Outside diameter [mm]	Inside diameter [mm]	Average wall thickness [mm]	Height [mm]
125.18	121.01	1.99-2.02	56.90	124.6-125.1	120.06-120.3	1.97-2.02	57.2-59.2

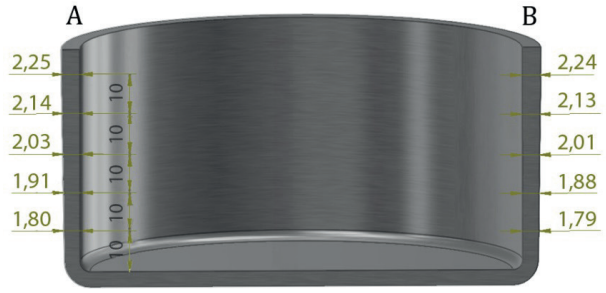

Fig. 6. Results of the experimental measurement of the wall's thickness. A, B – opposite sides of the product

The thickness distribution obtained from simulation and experimental studies are convergent. Minimal differences may be due to two factors:

1. The fixed value of the penalty stiffness of 10^4
2. The mechanical properties of the material used for purposes of numerical analysis.

4.2. Stage 2 – flow forming

The next stage of the investigation concerned numerical and experimental testing of flow forming process. The results of measurement of initially 2 mm thick drawpiece subjected to the flow forming are presented in Table 3.

The relative elongation of the product of flow forming was calculated according to formula:

$$\varepsilon_x = \frac{l - l_0}{l_0} \cdot 100\% \qquad (2)$$

where:

l_0 – height of the product before flow forming [mm]

l – height of the product after flow forming [mm]

Figure 7 shows the shape of the side wall of the drawpiece being in contact area with the roller and map of distribution of its thickness.. The comparison of theoretical and numerical wall thickness distributions after the elongative flow forming process is presented in Table 4. Figure 8 presents the distribution of side wall thicknesses of selected products graphically.

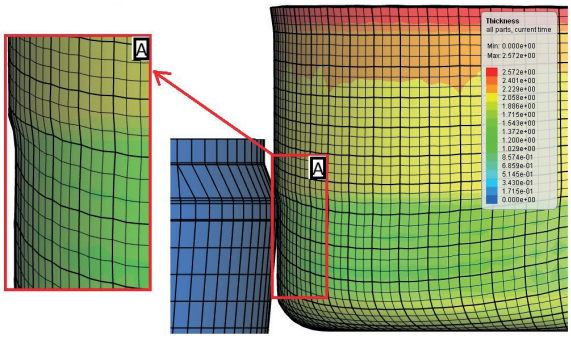

Fig. 7. The shape of the side wall of the workpiece being in contact with the roller and map of its thickness

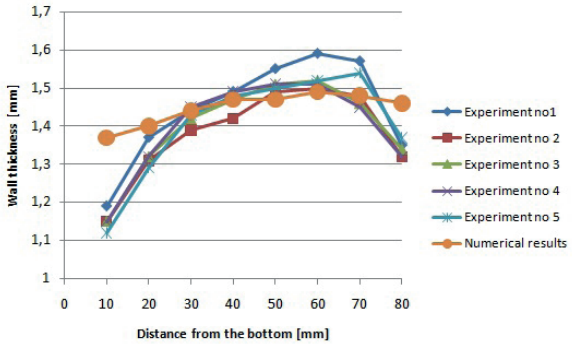

Fig. 8. Graphical presentation of the distribution of wall thicknesses of drawpiece after flow forming

TABLE 3

Results of measurements of the 2 mm thick products from Hastelloy C-276 after the first lengthening flow forming operation.

	Deformation in the direction of the wall's thickness [%]		**Average wall thickness [mm]**	**Height [mm]**	**Elongation [%]**
	planned	actual			
Experimental work	30	30.5 - 31	1.38 – 1.39	80.2 – 82.6	38.5-41.9
Numerical analysis	30	27-30.5	1.41 – 1.46	79.8 – 80.2	40.2 – 40.9

TABLE 4

Wall thickness on the side wall of the product after flow forming

ProductNo.	**Distance from the bottom of the product.**								**Average wall thickness**
	10	20	30	40	50	60	70	80	
NUMERICAL ANALYSIS									
1	1.37	1.40	1.44	1.47	1.47	1.49	1.48	1.46	1.44
EXPERIMENTAL TESTS									
1	1.19	1.37	1.44	1.49	1.55	1.59	1.57	1.35	1.44
2	1.15	1.31	1.39	1.42	1.49	1.50	1.48	1.32	1.38
3	1.15	1.32	1.42	1.47	1.51	1.52	1.46	1.34	1.4
4	1.15	1.32	1.45	1.49	1.51	1.51	1.45	1.32	1.4
5	1.12	1.29	1.43	1.48	1.50	1.52	1.54	1.37	1.41

The differences in thickness obtained from simulation and experiment for the points at the bottom of the product result from one of the assumption of numerical model. The tools used for simulation process were rigid, whilst during experimental studies they were subjected to deformation.

An increase in internal diameter of the product's upper part after the flow forming is observed. In case of numerical simulations, near the bottom of the product, the internal diameter was 120.4 mm, while in the upper part its value was equal to 122.7 mm. The corresponding experimental values lay in the ranges: 120.1 – 120.3 mm and 121.1–121.4 mm, respectively.

Figure 9 and 10 show the distribution of effective plastic strain in the deformation zone of the workpiece being in contact with the roller for both initial and final stages of the process, respectively. In the contact area the effective plastic strain value varies from 0.9 to 1.01 for initial stage and from 1.41 to 1.47 for final stage. Very small differences in thickness for such a large strain deformation in experimental tests may result from the difficulty of maintaining the rigidity of tools. The analysis performed in the Metal Forming Institute in Poznan showed serious difficulties in maintaining the stiffness of the tools, despite the linear transition of rollers in the process.

The shapes of the drawpieces being products of numerical simulation and experimental work, at final stages of both stamping and flow forming processes, are presented in Figures 11 and 12, respectively.

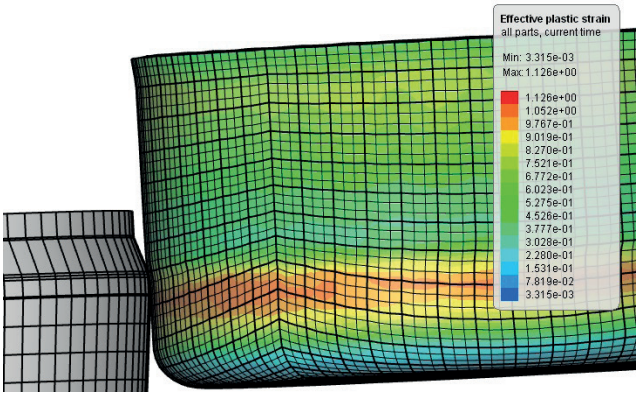

Fig. 9. The distribution of effective plastic strain for initial forming stage.

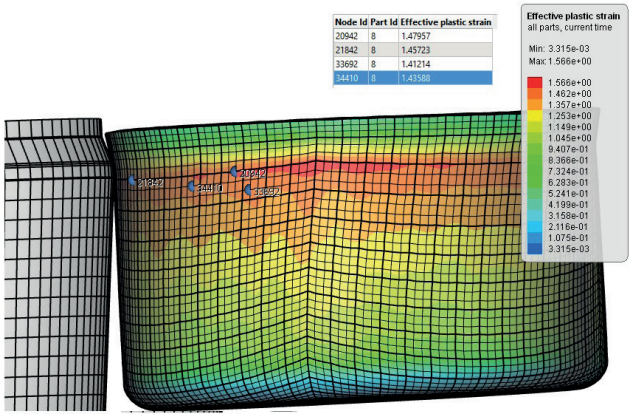

Fig. 10. The distribution of effective plastic strain for final forming stage.

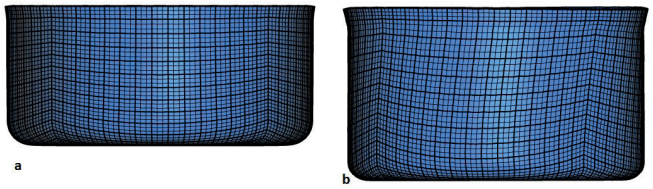

Fig. 11. Final shapes of products of numerical analysis, a) after stamping, b) after flow forming

Fig. 12. Final shapes of products of experimental work, a) after stamping, b) after flow forming

5. Conclusion

The paper presents results of numerical simulation and experimental investigation of axial-symmetrical drawpiece made by using two subsequent operations: deep drawing and flow forming. The simplified numerical model was used for purposes of the simulations. The lack of material anisotropy and yield stress curve computed on the basis of a material database were the main simplifications of the model. They were caused by the lack of real material properties.

The numerical model was also adjusted to work with rigid tools by application of a penalty-driven stiffness of the tool kit. The penalty factor value of 10^4 was adopted. This assumption results in the release of contact at the workpiece – tools interface. This method has two advantages in comparison to constraint based methods, where the surface has to be in perfect contact without any overlaps. The first one is the easy maintenance of energy balance. The second one is the easy use of complex contact models resulting in possibility of friction consideration and faster computation. Analysis of the numerical model suggests, that in order to increase the computation accuracy, penalty factor value has to be multiplied by 10.

The presented work concerning investigation of both the processes: stamping and flow forming of drawpieces made in Metal Forming Institute in Poznan, has provided positive results and shown the practical possibility of forming products made of hard-to deform alloys using the mentioned methods.

Despite the simplifications of the numerical model, verification of theoretical results in experimental studies have shown a very good convergence of both the methods. In the future work it is necessary to use a real stress-strain curve and material anisotropy in the numerical model which should allow to achieve even more accurate results.

Acknowledgements

1. The concept of the paper as well as the numerical analysis is the work done with financial support of AGH founds (grant no. 11.11.110.300).

2. The experimental work presented in the paper was realized within the research project No. N507 593838 in Metal Forming Institute in Poznań.

REFERENCES

[1] M. Hojny, Application of an integrated CAD/CAM/CAE/IBC system in the stamping process of a bathtub 1200S, Archives of Metallurgy and Materials, 55, 713 (2010).

[2] M. Hojny, M. Głowacki, A. Opaliński, D. Woźniak, Computer aided design of stamping process technology using the eta/DYNAFORM 5.8 system, Mechanika, 7, 170 (2011).

[3] D. Woźniak, M. Głowacki, M. Hojny, T. Pieja, Application of CAE systems in forming of drawpieces with use rubber-pad forming processes, Archives of Metallurgy and Materials, vol. 57 (4), 1179–1187 (2012).

[4] S. Frąckowiak, Projektowanie procesów technologicznych wytłoczek osiowosymetrycznych na wyoblarkach sterowanych CNC, Obróbka Plastyczna Metali, t.XXII nr 1, 45-56 (2011).

[5] T. Drenger, J. Wiśniewski, J. Lisowski, T. Gądek, S. Frąckowiak, Ł. Nowacki, Doskonalenie technologii kształtowania obrotowego wyrobów złożonych, Obróbka Plastyczna Metali, t.XX nr 2, 66-86 (2010).

[6] S. Hamilton, H. Long, Analysis of conventional spinning process of a cylindrical part using finite element method, Steel research international, 79 (1), 632-639 (2008).

[7] Chun-Ho Liu, A-Cheng Wang, Kuo-Zoo Liang, Sheng-En Hsu, Analysis of Conventional Spinning Process with Thermal Effects, Materials Science Forum, Vol. 594, 187-192 (2008).

[8] G. Sebastiani, A. Brosius, W. Homberg, M. Kleiner, Process Characterization of Sheet Metal Spinning by Means of Finite Elements, Key Engineering Materials Vol. 344, 637-644, (2007).

[9] N. Alberti, L. Fratini: Innovative sheet metal forming processes: numerical simulations and experimental tests, Journal of Materials Processing Technology 150, 2-9 (2004).

[10] M.H. Parsa, A.M.A. Pazooki, M. Nili Ahmadabadi, Flow-forming and flow formability simulation, Int J Adv Manuf Technol 42, 463–473 (2009).

[11] A. Szummer, K. Lublinska, Wpływ odkształcenia plastycznego na dyfuzję wodoru w odpornych na korozję stopach niklu, Inżynieria Materiałowa, nr 1, 23-28 (2006).

[12] T. Gądek, Badanie możliwości kształtowania stopu Hastelloy C276 metodą tłoczenia oraz zgniatania obrotowego, Obróbka Plastyczna Metali, nr 1, 31-44 (2011).

[13] A.J. Walter i inni: Eksperimantalnoe issledovanie mahanizma deformacji psi potacionnoj rytazke. Kuzneczno-sztampowocznoje proizwostwo, nr 9, 9-11 (2004).

[14] C. Malanna i inni: Process parameters in flow forming and how they affect the and product. Proc. Ist Ins. Conf. Rotary Metalwork Process, Londyn, Kempston 1979, s.229, 231-242 (1979).

[15] T. Drenger, J. Wiśniewski. Badania technologii miejscowego zgniatania obrotowego wyrobów rurowych. Badania procesu zgniatania obrotowego wydłużającego rur dla materiałów R-35 i R-45. Praca niepublikowana.

[16] T. Drenger, J. Wiśniewski, J. Lisowski, T. Gądek, S. Frąckowiak, Ł. Nowacki Doskonalenie technologii kształtowania obrotowego wyrobów złożonych. Obróbka Plastyczna Metali t. XX nr 2, 22-35 (2009).

Received:20 March 2015.